

# Characterization of thermally induced of crystalline phases in CuO-containing silicate–phosphate glasses

Justyna Sułowska · Irena Waclawska ·  
Magdalena Szumera · Zbigniew Olejniczak

MEDICTA2011 Conference Special Chapter  
© Akadémiai Kiadó, Budapest, Hungary 2011

**Abstract** The DSC, XRD, FTIR, and  $^{31}\text{P}$  MAS-NMR methods were applied to study complex crystallization processes occurring during the thermal treatment of multicomponent  $\text{SiO}_2\text{--P}_2\text{O}_5\text{--K}_2\text{O--CaO--MgO}$  glasses modified by the addition of variable amount of copper. The crystallization temperatures were found to decrease with the increasing copper content. The products of multistage crystallization identified by XRD and characterized by FTIR and NMR are the  $\text{Ca}_9\text{KMg}(\text{PO}_4)_7$  and  $\text{Ca}_{19}\text{Cu}_2(\text{PO}_4)_{14}$  phosphates of whitlockite-type, and the  $\text{CaMgSi}_2\text{O}_6$  and  $\text{Cu}_{0.69}\text{Mg}_{1.31}\text{Si}_2\text{O}_6$  silicates of diopside type.

**Keywords** Crystallization · Silicate–phosphate glasses · CuO · XRD · FTIR ·  $^{31}\text{P}$  MAS-NMR

## Introduction

The silicate–phosphate glasses from the  $\text{SiO}_2\text{--P}_2\text{O}_5\text{--K}_2\text{O--CaO--MgO}$  system started recently to be used as ecological fertilizers providing controlled release rate of the macroelements (P, Ca, K, and Mg) for plants [1, 2]. This type of glass shows also the capability of receiving to their composition a series of elements acting as microelements (B, Fe, Zn, and Cu).

The chemical activity of such glasses in the soil environment depends on the type and amount of components forming the glass network and the location of additives. Therefore, the detailed knowledge of the microscopic structure is of crucial importance for designing materials with optimal structure–properties relationship for a given application.

Earlier studies showed that the introduction of boron [3] or iron [4] into the structure of silicate–phosphate glass causes the formation of chemically stable P–O–B and P–O–Fe bonds, respectively, decreasing the glass solubility in the soil environment. It was also found that the ability for crystallization, its course, and the type of the resulted crystalline phases depend on relative proportions between the  $\text{B}_2\text{O}$  or  $\text{Fe}_2\text{O}_3$  and  $\text{P}_2\text{O}_5$  units forming the glass structure. These proportions correspond to the character of domains present in the glass structure.

The subject of the present studies were the silicate–phosphate glasses from the  $\text{SiO}_2\text{--P}_2\text{O}_5\text{--K}_2\text{O--CaO--MgO}$  system modified by the addition of copper, which is one of the microelements that plays an important role in the growth of plants. In order to determine the role of copper in the structure and properties of these glasses, a detailed study of the course of crystallization were carried out. From these results, the amorphous structure of the materials can be inferred, because it is similar to the structure of their devitrificates.

J. Sułowska (✉) · I. Waclawska · M. Szumera  
Faculty of Materials Science and Ceramics, AGH University of  
Science and Technology, Mickiewicza 30, 30-059 Cracow,  
Poland  
e-mail: sulowska@agh.edu.pl

Z. Olejniczak  
Institute of Nuclear Physics, Polish Academy of Sciences,  
Radzikowskiego 152, 31-342 Cracow, Poland

## Experimental

A series of silicate–phosphate glasses from the  $\text{SiO}_2\text{--P}_2\text{O}_5\text{--K}_2\text{O--MgO--CaO--CuO}$  system with variable contents of CuO was prepared. Keeping the  $\text{K}_2\text{O}$  and  $\text{SiO}_2$  constant, an increasing amount of CuO was introduced at the cost of

MgO and CaO, with the constant MgO/CaO ratio. The samples were produced by melting the mixture of raw materials, i.e., SiO<sub>2</sub>, H<sub>3</sub>PO<sub>4</sub>, MgO, CaCO<sub>3</sub>, and CuO at the temperature of 1450 °C. Then the batch-free glasses were fritted in water and grinded to the grain size of 0.1–0.3 mm. The actual chemical composition of synthesized glasses was determined by the X-ray fluorescence spectrometry (XRF) method, and is presented in the Table 1.

The thermal stability of glasses was determined by the differential scanning calorimetry (DSC) measurements conducted on the STA 449 F1 Jupiter (Netzsch) apparatus, operating in the heat flux DSC mode. The 60 mg samples were heated to 1100 °C in the platinum crucibles at the rate of 10 °C/min in a dry nitrogen atmosphere. The glass transformation temperature  $T_g$  and the crystallization temperature  $T_C$  were determined as the midpoint of the change in the specific heat  $C_p$  in the glass transformation region, and as the onset of the first crystallization peak, respectively. The Netzsch Proteus Thermal Analysis program (version 5.0.0) was used to evaluate the thermal parameters of the glasses.

The X-ray diffraction (XRD) method using the X'Pert PRO Diffractometer (Philips) was applied to confirm the amorphous state of the synthesized glasses, and the results are also shown in the Table 1.

The fourier transform infrared (FTIR) studies were carried out on the Digilab FTS60s spectrometer in MIR range (400–4000 cm<sup>-1</sup>). The samples were prepared in the form of KBr pellets.

The <sup>31</sup>P MAS-NMR spectra were measured using the APOLLO console (Tecmag) and the 7 T/89 mm superconducting magnet (Magnex). A Bruker HP-WB high speed MAS probe equipped with the 4 mm zirconia rotor and the KEL-F cap was used to spin the sample at 8 kHz. The resonance frequency was equal to 121.264 MHz, and a single 3 μs rf pulse, corresponding to  $\pi/2$  flipping angle was applied. The acquisition delay in accumulation was 30 s, and 128 scans were acquired. The frequency scale in ppm was referenced to the <sup>31</sup>P resonance of 85% mol H<sub>3</sub>PO<sub>4</sub>.

The samples were isothermally heated for about 5 h at the crystallization temperatures that were inferred from the

DSC measurements. The temperature stability was better than  $\pm 5$  °C. The resulted crystalline phases were detected and identified by XRD, FTIR, and <sup>31</sup>P MAS-NMR.

## Results and discussion

The DSC curves of the analyzed samples are shown in Fig. 1. They clearly illustrate the multistage crystallization processes occurring in these glasses. Depending on the glass composition, the number of exothermic peaks ranges from four to five. Typically, three to four narrow low-temperature peaks appearing in a relatively small temperature range are followed by a broad, high-temperature peak, which is characterized by a large heat of reaction. An exception is the 6.5Cu sample, where only four narrow peaks are observed. The temperature of first crystallization decreases with the increasing copper content. The numerical results of the thermal analysis are presented in the Table 2. In the case of overlapping exothermic effects, as for the 2.5Cu and 5Cu samples, it was impossible to obtain the values of reaction heat corresponding to individual peaks. The data for the 35Cu sample is not included in the table, because it was already crystalline as synthesized.

Separate samples of analyzed glasses were isothermally heated for 5 h at all crystallization temperatures that were found by DSC. They represented the consecutive steps of crystallization, although corresponding exothermic peaks partially overlap (Fig. 1). The XRD measurements showed, however, that for a given glass composition, the products of crystallizations were identical in the samples heated at close temperatures. Therefore, the Table 2 shows the XRD results for two or three temperature ranges, characterized by the same crystalline phases.

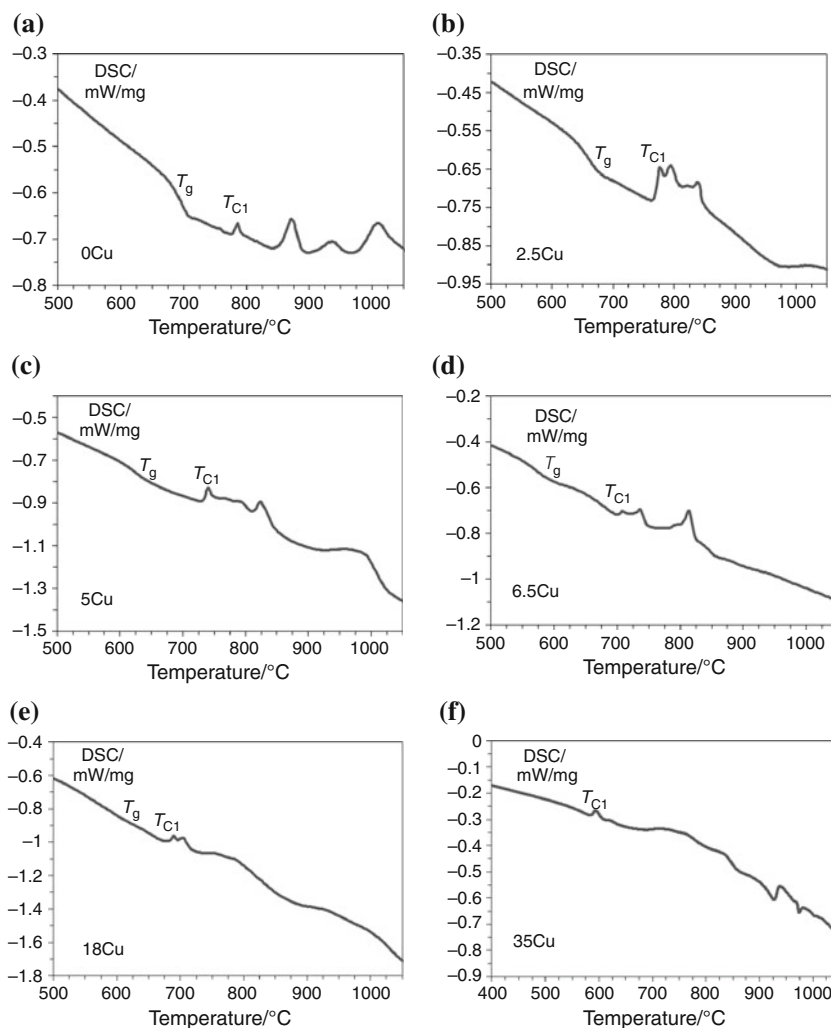
In the copper-free sample (0Cu), the XRD identified a mixed calcium–magnesium–potassium orthophosphate Ca<sub>9</sub>MgK(PO<sub>4</sub>)<sub>7</sub> in the 750–900 °C temperature range, while at higher temperatures an additional crystalline phase of the diopside type appeared.

In all analyzed samples containing copper, a single crystalline phase of calcium–copper phosphate Ca<sub>19</sub>Cu<sub>2</sub>(PO<sub>4</sub>)<sub>14</sub>

**Table 1** The chemical composition of the silicate–phosphate glasses from the SiO<sub>2</sub>–P<sub>2</sub>O<sub>5</sub>–K<sub>2</sub>O–MgO–CaO–CuO system

| Glass name | Chemical composition/mol % |                               |                  |      |      |      | State of material     |
|------------|----------------------------|-------------------------------|------------------|------|------|------|-----------------------|
|            | SiO <sub>2</sub>           | P <sub>2</sub> O <sub>5</sub> | K <sub>2</sub> O | CaO  | MgO  | CuO  |                       |
| 0Cu        | 42.6                       | 6.5                           | 6.7              | 23.0 | 21.2 | –    | Amorphous             |
| 2.5Cu      | 42.6                       | 6.4                           | 6.7              | 22.8 | 19.0 | 2.5  | Amorphous             |
| 5Cu        | 43.0                       | 6.5                           | 6.9              | 20.3 | 18.4 | 4.9  | Amorphous             |
| 6.5Cu      | 40.0                       | 7.0                           | 6.3              | 16.8 | 23.9 | 6.4  | Amorphous             |
| 18Cu       | 41.7                       | 6.1                           | 6.4              | 14.6 | 12.9 | 18.3 | Partially crystalline |
| 35Cu       | 37.5                       | 5.3                           | 6.0              | 7.7  | 8.4  | 35.2 | Crystalline           |

**Fig. 1** DSC curves of **a** 0Cu, **b** 2.5Cu, **c** 5Cu, **d** 6.5Cu, **e** 18Cu, and **f** 35Cu glasses



was identified in the low temperature range, except for the 18Cu sample, in which copper oxide of tenorite type crystallizes first. On the other hand, the additional crystalline phases that appear at the high-temperature range are identical to the phases found in the copper-free sample. Again the exceptions are the samples with high copper content (6.5Cu and 18Cu), in which the CuO crystalline phase dominates. Three separate temperature ranges characterized by different crystalline phase compositions were found in the sample with highest copper content (18Cu). A non-stoichiometric copper–magnesium silicate of the diopside type ( $\text{Cu}_{0.69}\text{Mg}_{1.31}\text{Si}_2\text{O}_6$ ) was identified in this sample at the highest temperature. A detailed analysis of structural transformations occurring in these materials during crystallization is beyond the scope of this article.

Based on the DSC and XRD results that were presented above, the following spectroscopic analyses by FTIR and NMR techniques were carried out on selected samples that were chosen to represent all temperature ranges at all glass compositions, for which the interesting crystalline phases were identified. The temperatures at which these samples

were prepared were set in the centers of the temperature ranges to assure their stability and are given as the extensions of the samples names.

The FTIR spectra of silicate–phosphate glasses modified by CuO measured in the middle infrared (MIR) range are presented in Fig. 2a, b, for samples crystallized in the low and high-temperature range, respectively. The spectra obtained at low temperatures (Fig. 2a) are practically identical, displaying the same character and position of the absorption bands. The bands located in the 1000–1120 and 600–400  $\text{cm}^{-1}$  ranges are characteristic for the whitlockite-type mixed calcium–magnesium–phosphate  $\text{Ca}_9\text{MgK}(\text{PO}_4)_7$  [5], which confirms the XRD result obtained for the 0Cu sample. On the other hand, the calcium–copper phosphate ( $\text{Ca}_{19}\text{Cu}_2(\text{PO}_4)_{14}$ ) phase that was found by XRD in the copper-containing samples is not visible in FTIR, because its characteristic absorption bands overlap with the whitlockite-type orthophosphates bands [5].

Additional absorption bands that are observed in the FTIR spectra of samples 0Cu, 2.5Cu, and 5Cu prepared in the high-temperature range (Fig. 2b) originate from the

**Table 2** Results of thermal and XRD analysis of silicate–phosphate glasses

| Glass name | $T_C/^\circ\text{C}$ | $\Delta H_C/\text{J/g}$ | Temperature range/ $^\circ\text{C}$ | Crystalline phase  |
|------------|----------------------|-------------------------|-------------------------------------|--|
| 0Cu        | 786                  | 2.0                     | 750–900                             | $\text{Ca}_9\text{MgK}(\text{PO}_4)_7$   |
|            | 872                  | 8.0                     |                                     |  |
|            | 935                  | 4.0                     | 900–1100                            | $\text{Ca}_9\text{MgK}(\text{PO}_4)_7$ , $\text{CaMgSi}_2\text{O}_6$   |
|            | 1010                 | 15.0                    |                                     |  |
| 2.5Cu      | 777                  | n.a.                    | 750–850                             | $\text{Ca}_{19}\text{Cu}_2(\text{PO}_4)_{14}$  |
|            | 795                  |                         |                                     |  |
|            | 822                  |                         |                                     |  |
|            | 838                  |                         |                                     |  |
| 5Cu        | 1030                 | 7.5                     | 950–1100                            | $\text{Ca}_{19}\text{Cu}_2(\text{PO}_4)_{14}$ , $\text{Ca}_9\text{MgK}(\text{PO}_4)_7$ , $\text{CaMgSi}_2\text{O}_6$ |
|            | 740                  | n.a.                    | 730–840                             | $\text{Ca}_{19}\text{Cu}_2(\text{PO}_4)_{14}$  |
|            | 771                  |                         |                                     |  |
|            | 793                  |                         |                                     |  |
| 6.5Cu      | 824                  |                         |                                     |  |
|            | 988                  | 42.0                    | 900–1010                            | $\text{Ca}_{19}\text{Cu}_2(\text{PO}_4)_{14}$ , $\text{Ca}_9\text{MgK}(\text{PO}_4)_7$ , $\text{CaMgSi}_2\text{O}_6$ |
|            | 736                  | n.a.                    | 700–850                             | $\text{Ca}_{19}\text{Cu}_2(\text{PO}_4)_{14}$ , CuO  |
|            | 792                  |                         |                                     |  |
| 18Cu       | 814                  |                         |                                     |  |
|            | 836                  |                         |                                     |  |
|            | 690                  | n.a.                    | 680–720                             | CuO  |
|            | 705                  |                         |                                     |  |
|            | 788                  | 32.8                    | 720–860                             | $\text{Ca}_{19}\text{Cu}_2(\text{PO}_4)_{14}$ , CuO  |
|            | 933                  | 48.6                    | 860–1050                            | $\text{Ca}_{19}\text{Cu}_2(\text{PO}_4)_{14}$ , $\text{Cu}_{0.69}\text{Mg}_{1.31}\text{Si}_2\text{O}_6$              |

$T_C$  crystallization temperature,  $\Delta H_C$ —heat of reaction, *n.a.* not available

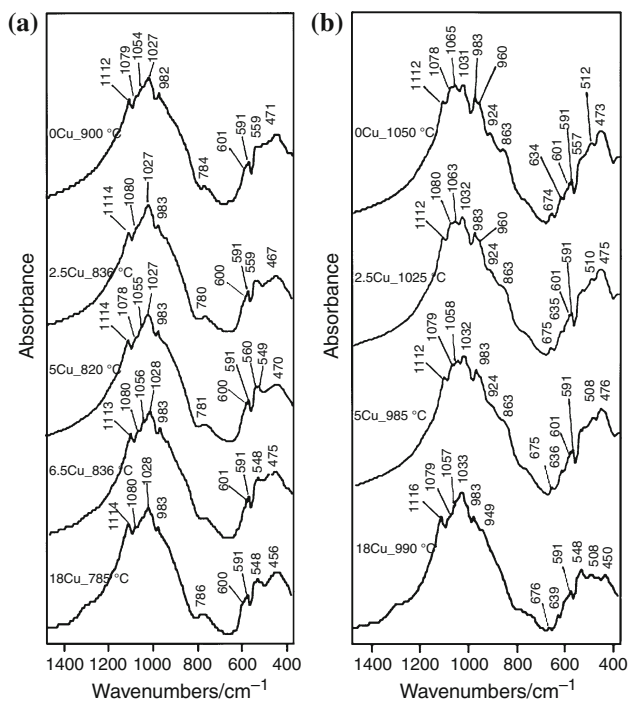


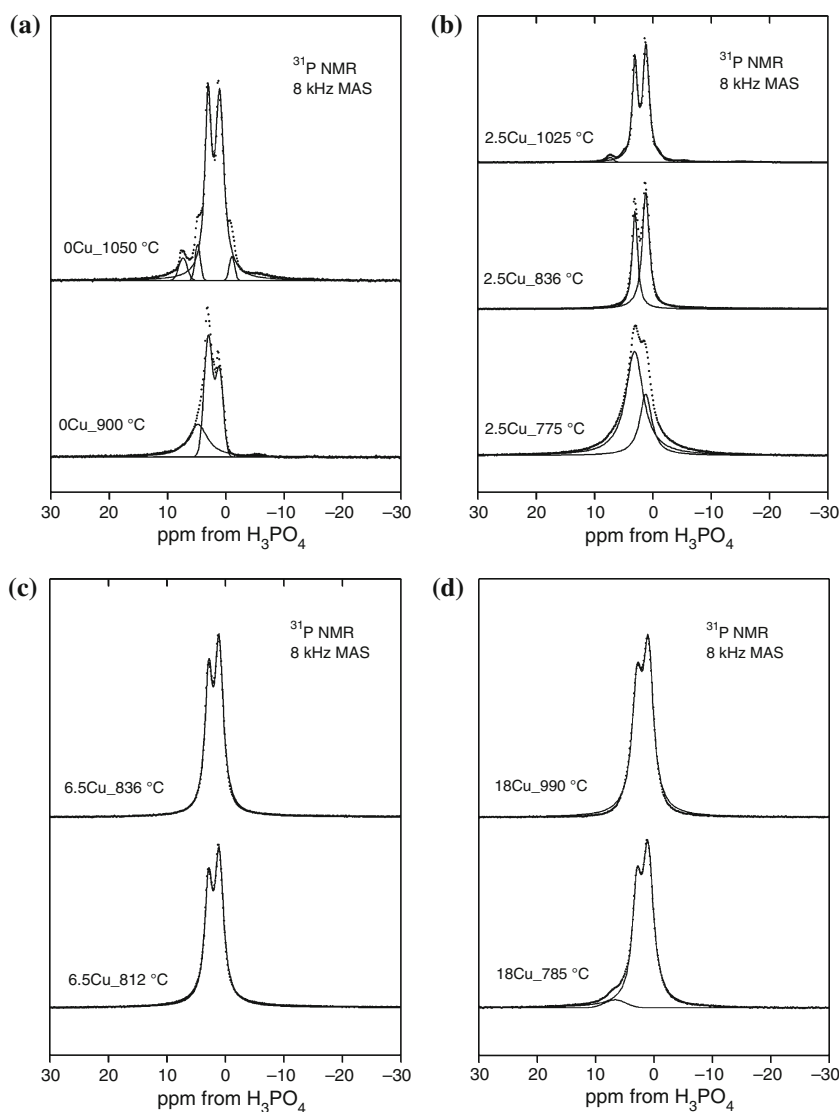
**Fig. 2** The FTIR spectra of silicate–phosphate glasses crystallized in **a** low and **b** high-temperature ranges

calcium–magnesium–silicate of the diopside type [6–8]. They are not observed in the 6.5Cu sample (not shown). The bands characteristic of diopside phase that are located at 960, 924, 863, 634, and 512  $\text{cm}^{-1}$  are clearly visible, while the bands at 1070  $\text{cm}^{-1}$  overlap with the absorption bands assigned to the orthophosphate phases. In the FTIR spectrum of the 18Cu\_990  $^\circ\text{C}$  sample, the bands at 960 and 924  $\text{cm}^{-1}$  are missing. They represent the vibrational modes of Si–O bonds in the diopside phase. Instead, a new band at 949  $\text{cm}^{-1}$  appears which may be attributed to the Si–O bonds in the silicate of  $\text{Cu}_{0.69}\text{Mg}_{1.31}\text{Si}_2\text{O}_6$  type. These findings agree well with the XRD results.

The  $^{31}\text{P}$  MAS-NMR spectra of recrystallized glasses from the  $\text{SiO}_2\text{--P}_2\text{O}_5\text{--K}_2\text{O--CaO--MgO}$  system containing different amount of copper are presented in the Fig. 3. In contrast to XRD and FTIR data, the MAS-NMR spectra are shown for each glass composition separately, to illustrate their evolution with temperature. The parameters of observed peaks, i.e., their positions and widths that were obtained from the deconvolution procedures are listed in the Table 3. The uncertainty of the peaks positions is about  $\pm 0.1$  ppm.

In general, narrow peaks dominate the  $^{31}\text{P}$  MAS-NMR spectra of thermally treated glasses, representing a high structural order of crystalline phases present in the samples.

**Fig. 3**  $^{31}\text{P}$  MAS-NMR spectra of **a** 0Cu, **b** 2.5Cu, **c** 6.5Cu, and **d** 18Cu devitrificates, experimental (dotted), and deconvoluted (solid)



In spite of limited frequency resolution of the technique, a systematic narrowing of the crystalline peaks with increasing temperature is observed in all samples, reflecting an increasing ordering of the phase. The residual broad peaks appearing in some spectra correspond to the amorphous, not completely recrystallized phase, and they will be omitted in the following analysis.

The  $^{31}\text{P}$  MAS-NMR spectra of copper-free (0Cu) glass display two narrow, equal intensity peaks at +3.2, +1.4 ppm and at +3.2, +1.2 ppm, for samples crystallized at the low and high temperature, respectively. In addition, narrow peaks of small intensities appearing in the spectrum of the 0Cu\_1050 °C sample at +7.5, +5.0, and -0.9 ppm represent some crystalline phases of unknown composition. According to the XRD and FTIR results, both samples should exhibit a single phosphorus-containing crystalline phase, namely, the  $\text{Ca}_9\text{MgK}(\text{PO}_4)_7$  phosphate. Therefore, the two peaks observed in the MAS-NMR spectra at +3.2,

+1.3 ppm (the average of +1.2 and +1.4 ppm) can be safely assigned to phosphorus atoms in this compound, occupying two chemically inequivalent sites of orthophosphate coordinations with equal concentrations.

Although the  $^{31}\text{P}$  MAS-NMR data for the calcium–magnesium–potassium phosphate of whitlockite-type ( $\text{Ca}_9\text{MgK}(\text{PO}_4)_7$ ) are not available in the literature, and the present results can be compared to the reported chemical shifts of simple orthophosphates, namely,  $\text{Ca}_3(\text{PO}_4)_2$ ,  $\text{Mg}_3(\text{PO}_4)_2$ , and  $\text{K}_3\text{PO}_4$ , equal to +3.0, +4.6, and +11.7 ppm, respectively [9]. The observed discrepancy can be explained by high sensitivity of  $^{31}\text{P}$  chemical shift to local bond geometry, chemical surrounding, and the electronegativity of neighboring cations [9].

According to the XRD results, the copper-containing samples treated at lower temperatures should exhibit a single crystalline calcium–copper phosphate ( $\text{Ca}_{19}\text{Cu}_2(\text{PO}_4)_{14}$ ) phase. The presence of such phase was not

**Table 3**  $^{31}\text{P}$  MAS-NMR parameters of CuO-containing recrystallized silicate–phosphates

| Glass name   | Chemical shift/ppm | FWHM/ppm | Glass name    | Chemical shift/ppm | FWHM/ppm |
|--------------|--------------------|----------|---------------|--------------------|----------|
| 0Cu_900 °C   | +4.9               | 4.5      | 2.5Cu_1025 °C | +7.5               | 1.5      |
|              | +3.2               | 1.7      |               | +3.2               | 1.0      |
|              | +1.4               | 1.5      |               | +1.4               | 1.3      |
|              | −4.9               | 3.8      | 6.5Cu_812 °C  | +3.0               | 1.6      |
| 0Cu_1050 °C  | +7.5               | 1.7      | 6.5Cu_836 °C  | +1.2               | 1.8      |
|              | +5.0               | 1.1      |               | +3.0               | 1.5      |
|              | +3.2               | 1.3      |               | +1.2               | 1.7      |
|              | +1.2               | 1.7      | 18Cu_785 °C   | +6.8               | 4.3      |
| 2.5Cu_775 °C | +3.3               | 3.6      | 18Cu_990 °C   | +3.1               | 1.9      |
|              | +1.4               | 2.5      |               | +1.2               | 2.2      |
| 2.5Cu_836 °C | +3.2               | 1.1      |               | +3.1               | 2.1      |
|              | +1.4               | 1.4      |               | +1.1               | 2.1      |

*FWHM* full width at half maximum

confirmed by FTIR, due to the overlap of its characteristic absorption bands with the whitlockite-type orthophosphates bands. A similar situation seems to occur in the case of NMR data for the 2.5Cu\_836, 6.5Cu\_812, 6.5Cu\_836, and 18Cu\_785 °C samples, in which the dominating narrow peaks occur in average at +3.1 and +1.3 ppm. These positions, within the stated accuracy, are identical to the ones observed in the copper-free samples, and were assigned to the  $\text{Ca}_9\text{MgK}(\text{PO}_4)_7$  phase. In the samples containing larger amount of copper (6.5Cu\_812, 6.5Cu\_836, and 18Cu\_785 °C), the lack of additional peaks could be explained by the presence of the CuO phase (see Table 2). However, since the XRD does not provide any quantitative information about the relative concentrations of observed crystalline phases, this is not conclusive.

The only indirect indication of the presence of additional crystalline phase in the copper-containing glasses is the asymmetry of the doublet that is observed in all corresponding  $^{31}\text{P}$  MAS-NMR spectra. The low-field peak at +1.3 ppm is systematically higher, which could be caused by the overlap of another peak originating from another phase. Again, this is not conclusive, because the asymmetry occurs in the spectra of samples treated at both low and high temperature, which, according to XRD, should consist of one and two different phosphorus-containing phases, respectively.

It follows from the above discussion that the  $\text{Ca}_9\text{MgK}(\text{PO}_4)_7$  and  $\text{Ca}_{19}\text{Cu}_2(\text{PO}_4)_{14}$  crystalline phases cannot be distinguished by the  $^{31}\text{P}$  MAS-NMR technique. This may be due to the coincidence of corresponding peaks, just like in the FTIR case. In principle, the application of  $^{63,65}\text{Cu}$  NMR spectroscopy could help in resolving the question. However, both copper nuclei have quadrupolar moments and the quadrupolar interaction

dominates, which makes the spectra less sensitive to the subtleties of microscopic structure. Moreover, a high resolution technique, like MQMAS would need to be applied, which is rather insensitive, so it limits the possible experiments to samples with high copper content. Nevertheless, such experiments are under preparation and, if successful, the results will be reported in the separate publication.

## Conclusions

Complex multistage crystallization processes induced by the thermal treatment in the multicomponent  $\text{SiO}_2\text{--P}_2\text{O}_5\text{--K}_2\text{O--MgO--CaO--CuO}$  glasses with variable copper content were characterized by the DSC method. The crystallization temperatures and heats of reactions were determined. The temperature of the first crystallization was found to decrease with the increasing copper content.

The resulted crystalline phases were identified by XRD as  $\text{Ca}_9\text{KMg}(\text{PO}_4)_7$  and  $\text{Ca}_{19}\text{Cu}_2(\text{PO}_4)_{14}$  phosphates of whitlockite-type and  $\text{CaMgSi}_2\text{O}_6$  and  $\text{Cu}_{0.69}\text{Mg}_{1.31}\text{Si}_2\text{O}_6$  silicates of diopside type, containing copper in their structure. The phosphate phases were found to crystallize at lower temperatures than the silicate phases. The compounds were also characterized by the FTIR and  $^{31}\text{P}$  MAS-NMR spectroscopic methods.

The results contribute to better understanding of microscopic structure of these materials and help in optimizing their properties in applications as ecological fertilizers with controlled solubility.

**Acknowledgements** This study was supported by the Polish Ministry of Science and Higher Education, Grant No. N R08 0010 06.

## References

1. Stoch L, Stoch Z, Waclawska I. Silicate glass fertilizer. Patent PL 185 229 B1. 2003.
2. Waclawska I, Szumera M. Reactivity of silicate–phosphate glasses in soil environment. *J Alloys Compd.* 2009;468:246–53.
3. Szumera M, Waclawska I, Olejniczak Z. Influence of B<sub>2</sub>O<sub>3</sub> on the structure and crystallization of soil active glasses. *J Therm Anal Calorim.* 2010;99:879–86.
4. Waclawska I, Szumera M, Stoch P, Sitarz M. Structural role of Fe in the soil active glasses. *Spectrochim Acta.* 2011;79:728–32.
5. Lazoryak BI, Khan N, Morozov VA, Belik AA, Khasanov SS. Preparation, structure determination, and redox characteristics of new calcium copper phosphates. *J Solid State Chem.* 1999;145: 345–55.
6. Farmer VC. The infrared spectra of minerals. In: *Minerological Society Monograph 4*. London; 1974
7. Omori K. Analysis of the infrared absorption spectrum of diopside. *Am Mineral.* 1971;56:1607–16.
8. Kalinkina EV, Kalinki AM, Forsling W, Makarov VN. Sorption of atmospheric carbon dioxide, structural changes of Ca, Mg silicate minerals during grinding: I. Diopside. *Int J Miner Process.* 2001; 61:273–88.
9. Turner GL, Smith KA, Kirkpatrick RJ, Oldfield E. Structure, cation effects on Phosphorous-31 NMR chemical shifts and chemical-shift anisotropies of orthophosphates. *J Magn Reson.* 1986;70:408–15.